Supporting Information for

Hydration Effect and Molecular Geometry Conformation as the Critical Factors Affect the Longevity Stability of G$_4$-structure-based Supramolecular Hydrogels

Jiang Liu,[a,#] **Lideng Cao,**[a,#] **Zheng Wang,**[a] **Qianming Chen,**[a] **Hang Zhao**[a,] **Xiurong Guo,**[b,]* **Yao Yuan,**[a,]*

[a]State Key Laboratory of Oral Diseases & National Center for Stomatology & National Clinical Research Center for Oral Diseases & Research Unit of Oral Carcinogenesis and Management & Chinese Academy of Medical Sciences, West China Hospital of Stomatology, Sichuan University, Chengdu 610041, Sichuan, China
[b]School of Pharmacy, Southwest Medical University, Luzhou 646000, Sichuan, China

[#]These authors contributed equally to this work.

*Correspondence:
Xiurong Guo
Email: xiurongguo@swmu.edu.cn
Yao Yuan
Email: yaoyuan_sklo@scu.edu.cn

Methods

General

α-8-aza-2'-deoxyguanosine (**αG$_d$***) was synthesized following the our previously published work.[1] Other chemicals were commercially available. The solvents and reagents were analytic pure, and all reagent water used in the laboratory was pretreated with the Milli-Q Plus System.

Crystallographic study

Single crystals were obtained by slowly cooling the corresponding saturated solution in steps of 0.5 °C h^{-1} from 100 to 30 °C. Proper-sized single crystals of compounds of **G$_d$, αG$_d$** and **αG$_d$***were stabilized into a tiny glass tube including mother liquor with epoxy resin to minimize solvent loss.

Hydrogels preparation

The powder of **G$_d$, G,** and **αG$_d$** was weighed and added to 0.2 M KCl solution and prepared to a concentration of 14 mg/ml, and then heated to 90 ℃ in a water bath until a clear and transparent solution was obtained. The heated solution was then cooled till the gel is obtained.

Rheology measurements

The measuring device was equipped with plate-plate geometry (25 mm in diameter, 1.0 mm gap) and a temperature unit (Peltier hood accessory), which offers temperature control. The viscoelastic behavior of hydrogel was analyzed by performing frequency sweep, strain sweep and shear thinning test. All measurements were conducted on hydrogel samples at concentrations of 14 mg/ml at 25 °C. Frequency sweep analysis was performed over an angular frequency (ω) of 0.1~100 rad·s^{-1}, under an initial strain (γ) of 0.1%. Strain-dependent rheology was conducted under γ from 0.1~100% at ω= 1 rad·s^{-1}. Shear thinning test was performed under a shear rate from 0.1~100 (1/s).

Circular Dichroism (CD)

CD spectrometer was performed using Chirascan V100 (Applied Photophysics, UK). **G$_d$, G, αG$_d$** and **αG$_d$*** in 0.2 M KCl with a concentration of 14 mg/ml. Then the CD

spectra were recorded between 220 and 320 nm, and the path length was 0.1 mm. The CD curve was further smoothed by using the Graphpad Prism 10.0. LD and UV-Vis spectra were measured under the identical conditions.

Powder X-ray Diffraction (PXRD)

X-ray Diffraction (PXRD) experiments were performed using Panalytical-Empyrean (Panalytical, Nederland). PXRD experiments were performed as described previously. Solid powder and hydrogel lyophilized powder were prepared as samples. The experiments were performed under the following conditions: the voltage and anode current used were 40 kV and 40 mA, and the radius was 240.00 mm. The active length was 3.3482°. And the diffractometer position was adopted as following, 2Theta = 9.9972°, Omega offset = 0.0000°, Z = 7.550 mm, respectively, the Cu Kα=1.540598 Å and scanning mode with 0.01° interval and 0.05 s of set time were used to collect the XRD pattern of samples and were recorded from 2° to 10° (SAXRD) or from 5° to 60°(WAXRD) (2θ).

Small-angle X-ray Scattering (SAXS) measurement

SAXS measurement capability was provided on the NanoStar instrument (Bruker, Germany) with Cu target (50Kv/50mA). Montel-P multilayer optics with pinhole collimation system provided the system for high flux/high resolution; Low background collimation system was using new SCATEX two-pinhole setup. The detector type was VÅNTEC-2000 2D. The softwares used in our study were SAXS for WindowsTM XP, DIFFRAC. SAXS and DIFFRAC. EVA. The exposure time was 30 min. The scattering intensity profile was output as the plot of the scattering intensity (I) vs the scattering vector, q = $(4\pi/\lambda) \sin(\theta/2)$ (θ = scattering angle). The samples were placed in a Hilgenberg quartz capillary with an outside diameter of 2 mm and a wall thickness of 0.01 mm.

Fluorescence measurement

Fluorescence intensity of ThT containing hydrogels was detected using Cary Eclipse (Agilent, USA). The emission spectra of G_4/ThT in the range of 450-600 nm with an excitationn wavelength of 450 nm.

Differential Scanning Calorimetry (DSC) measurements

DSC measurements were performed using a Universal V2.5H instrument (TA, America). The compounds were dissolved in 0.2M KCl solution, and heated to 90°C to transparent state, and then cooling down to room temperature to serve as the samples. For every experiment, the samples were first equilibrated to -60 °C and then heated at a rate of 5 °C/min in flowing N_2.

Low Field Nuclear Magnetic Resonance (LF-NMR) measurement

Transverse spin-spin relaxation (T_2) measurement was performed on a MesoMR23-060V-I NMR Analyzer (Niumag Co., Ltd., Shanghai, China) equipped with a 0.5 T permanent magnet, operated at 23.2 MHz for 1H-resonance frequency and 32 °C. Every sample was placed in a glass NMR tube which was inserted into a 40-mm diameter radio frequency coil to measure T_2 relaxation times. Then T_2 decay was measured by using the Carr-Purcell-Meiboom-Gill (CPMG) sequence with a τ value of 100 μs (intervals between the 90° and 180° and the 90° and 180° pulses of 13 and 26 μs, respectively).

Quantitative calculation

Conformational search was firstly carried out for the four structures (**G**, **G_d**, **$αG_d$**, **$αG_d$***) using B3LYP functional with D3(BJ) dispersion correction and 6-31G* basis set, with SMD solvation model in water solvent. The most stable four isomers were selected to construct the G-quartet blocks. Then the most stable G-quartet blocks were selected to further construct the supramolecular assemblies.

The four supramolecular assemblies' structures were optimized using the semi-empirical PM7 method. The recently developed PM7 semi-empirical method has included dispersion and hydrogen-bond corrections and allows a better description of noncovalent interactions, especially hydrogen-bonding. Moreover, PM7 is considered to be suitable for modeling a wide range of species. The single-point calculations were further improved by using B3LYP functional with D3(BJ) dispersion correction and 6-31G* basis set, with the SMD model (water as solvent) on the optimized geometries. All calculations were carried out with Gaussian 09.

Molecular Dynamics (MD) simulations

Gromacs 2019.6 package was used to perform all the MD simulation with periodic boundary conditions, applying the Amber14SB all-atom force field combining the TIP3P water model. Long-range electrostatics were calculated using the particle mesh Ewald method with 1.0 nm real space cutoff. For van der Waals interactions, a cutoff value of 1.0 nm was used. All hydrogen related bonds were constrained by the LINCS algorithm. The V-rescale method was used to control the system temperature to 300 K, and Parrinello-Rahman method was used to control the pressure to 1 bar. The three molecules collectively form nine systems (**G**, **G$_4$**, **G$_4$-10**, **G$_d$**, **G$_{d4}$**, **G$_{d4}$-10**, **αG$_d$**, **αG$_{d4}$**, **αG$_{d4}$-10**). The nine configurations were energy minimized and subjected to 100 ps NVT equilibration at 300 K. Then, the nine systems were run for 50 ns of NPT production respectively. The time step of simulation was 2 fs. The trajectories were saved every 10 ps, yielding a total of 5,000 snapshots for production analysis.

The crystal structures containing G$_4$-structures were downloaded from the PDB database, specifically selecting PDB ID 1XAV. Using the YASARA software, atoms were deleted and replaced to obtain structures containing one layer of G$_4$, G$_{d4}$, and αG$_{d4}$. Subsequently, the YASARA software was used to translate and rotate the single-layer structures to obtain structures with 10 layers. The distances and angles for translation and rotation were referenced from the previously literature.[2]

Cryo-SEM imaging

The hydrogels (1.4 wt%) were prepared by the methods above. Helios G4 UC cryogenic dual-beam scanning electron microscope is used. The sample was loaded into the sample holder and quickly plunged into pre-prepared slush nitrogen for about 1 minute for rapid freezing. The frozen fixed liquid sample is then transferred to the sample preparation chamber pre-cooled to -140°C using a Quorum cryogenic transfer device. In a vacuum and low-temperature environment, the sample is randomly fractured. The sample undergoes sublimation for 10 minutes at -70°C, followed by Pt conductive coating treatment for biological samples. The sample is then transferred to the cold stage of the Helios G4 UC cryogenic dual-beam scanning electron microscope's sample

chamber via a cryogenic transfer rod, and observations are made at a temperature of -140°C. Imaging is performed under working conditions of 5 kV voltage and 25 pA beam current.

Sustained-release experiment

Hydrogels were prepared according to the previously described method and methylene blue was added into it while in liquid form. Transfer the mixture into a glass bottle and allow it to naturally cool and set into a hydrogel. Add an equal volume of aqueous solution above the hydrogel as the receptor solution. Sample the receiving solution immediately after preparation, and at 1, 2, 4, and 24 hours. Use an UV-vis spectrophotometer to measure the concentration of methylene blue in the samples. Calculate the release curve based on these measurements.

Statistical analysis

All statistical analysis was performed by using the Graphpad Prism 10.0. Experiments were conducted in triplicates, or otherwise indicated. The data were presented as mean value ± SD (standard deviation) without pre-processing. Statistical comparisons between different groups were evaluated with two-way ANOVA test and repeated measures analysis of variance as summing significant at P-value < 0.05.
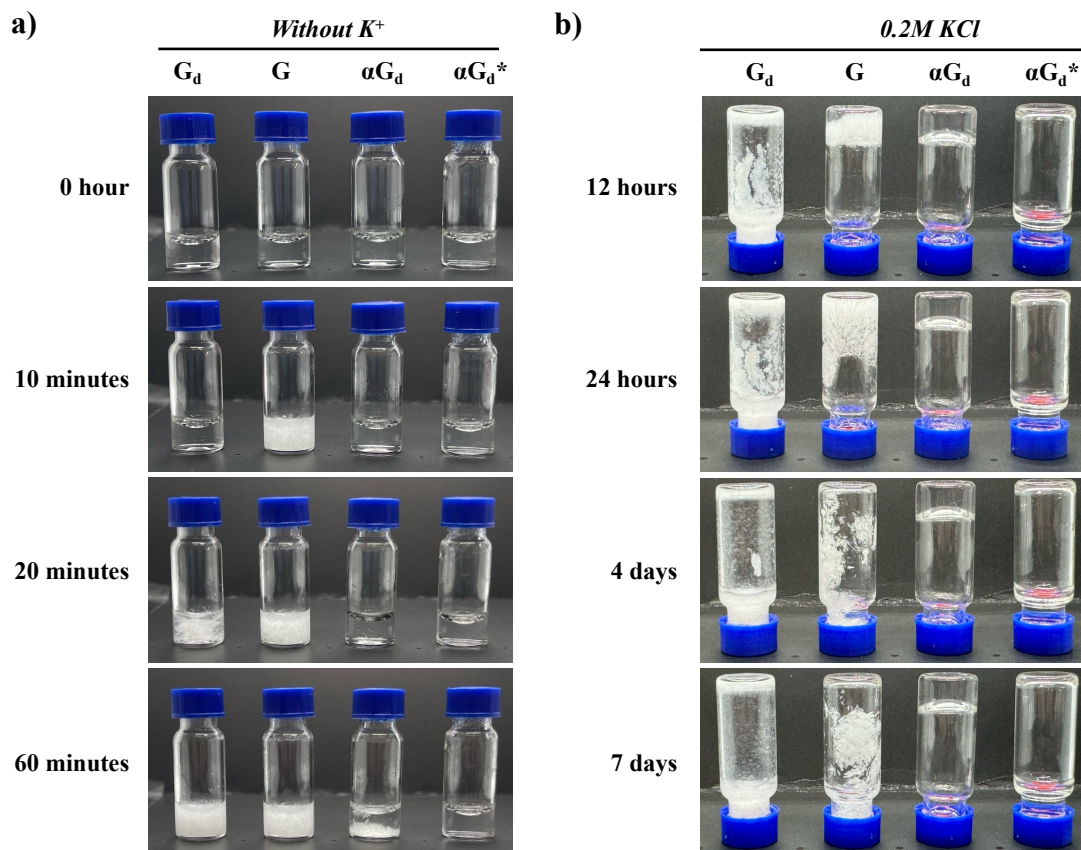
Figure S1. Hydrogel formation of guanosine compounds. a) none of guanosine compounds can form hydrogel in the absence of alkaline metal ions, and **G$_d$**, **G**, and **αG$_d$** gradually underwent precipitation and disintegration in 1 hour; b) **αG$_d$** can maintain its transparent gel state for more than 7 days.
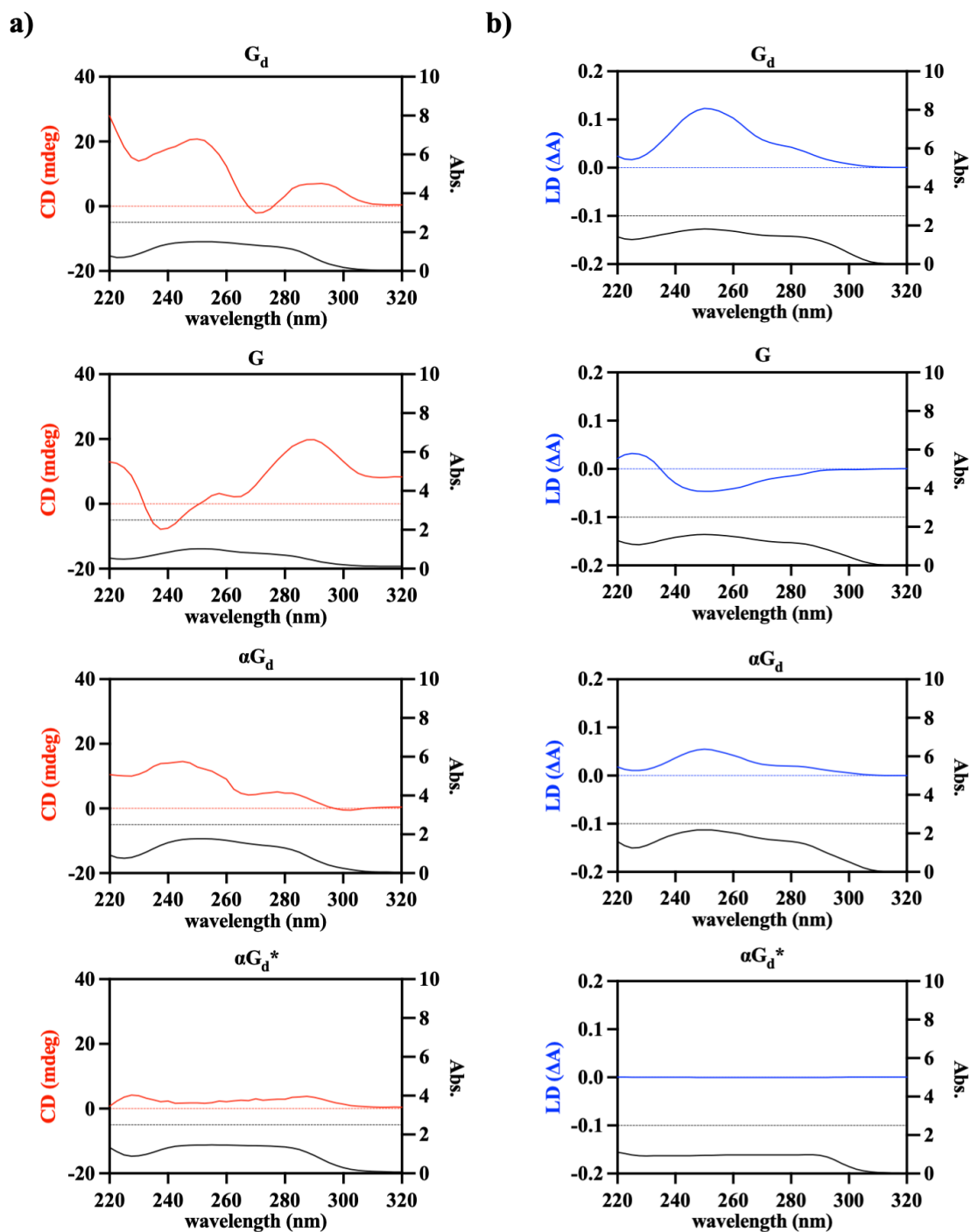
Figure S2. The CD, LD and UV-vis spectra of G_d, G, αG_d hydrogel and αG_d^* solution. a) CD and UV-vis spectra of each sample; b) LD and UV-vis spectra of each sample under the same conditions as the CD measurement. All absorbance values are <2.5 (black dotted line)
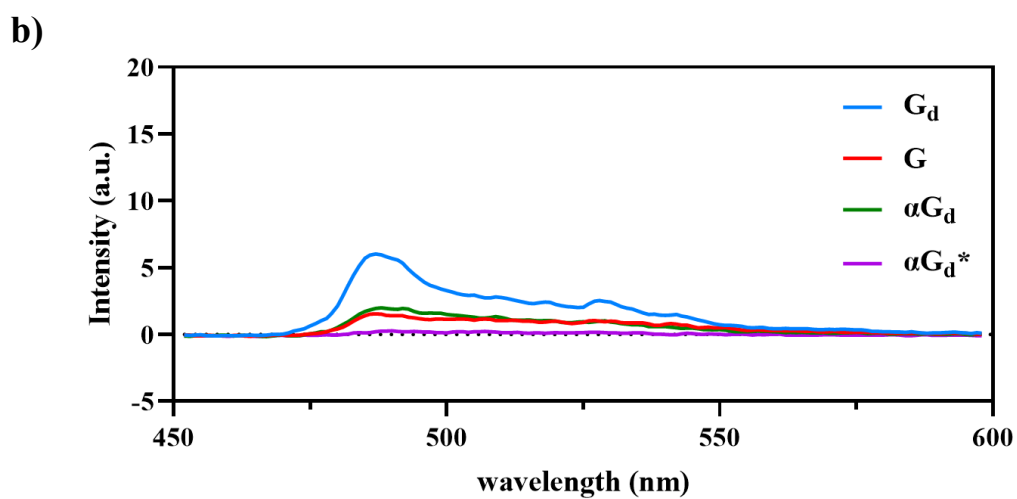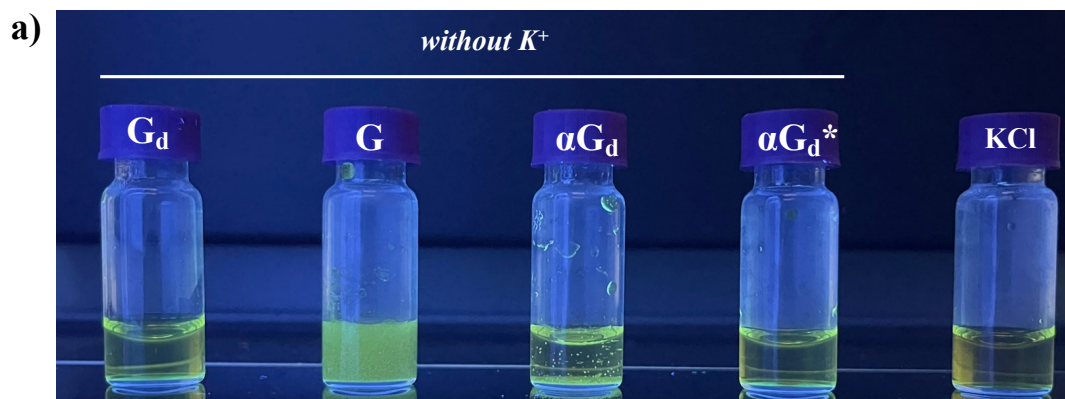
Figure S3. ThT-containing G_d, G, αG_d, and αG_d^* solution without K^+. a) Fluorescence was not observed in the absence of K^+ at 365 nm ultraviolet light irradiation, and G exhibited precipitation due to its instability. b) Compared to the presence of K^+, no significant fluorescence intensity was observed. The concentration of ThT is 5 mmol/mL, $\lambda_{ex} = 450$ nm.
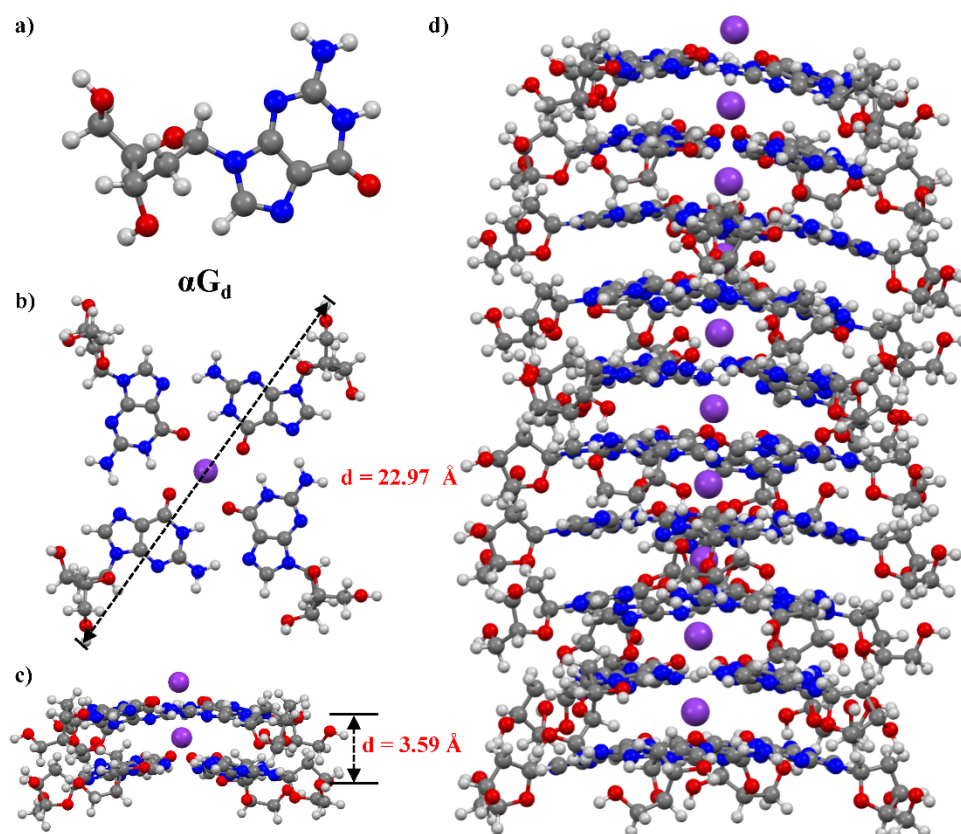
a)

G$_d$

b)

d = 23.64 Å

c)

d = 3.23 Å

d)
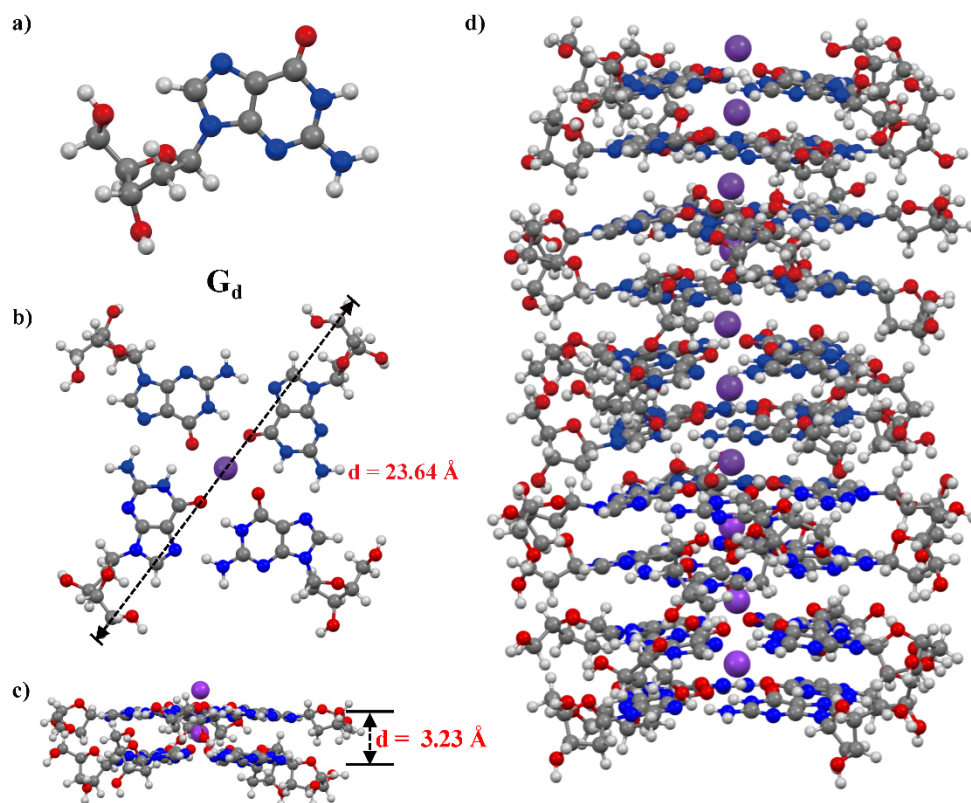
Figure S4. Structural modeling of various structures formed by **G$_d$**. a) the molecular structure of **G$_d$**. b) the G-quartet block structure under the mediation of potassium ions. c) the stacking structure formed by 2 layers of G-quartet blocks. d) the stacking structure composed of 10 layers of G-quartet blocks.
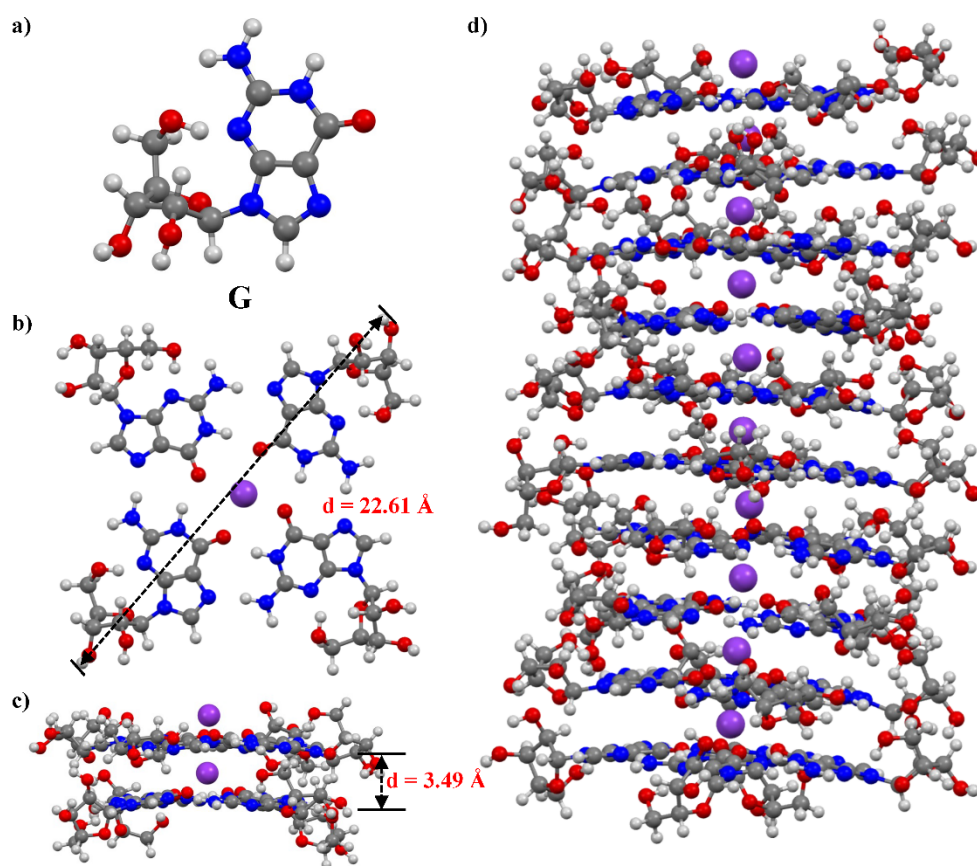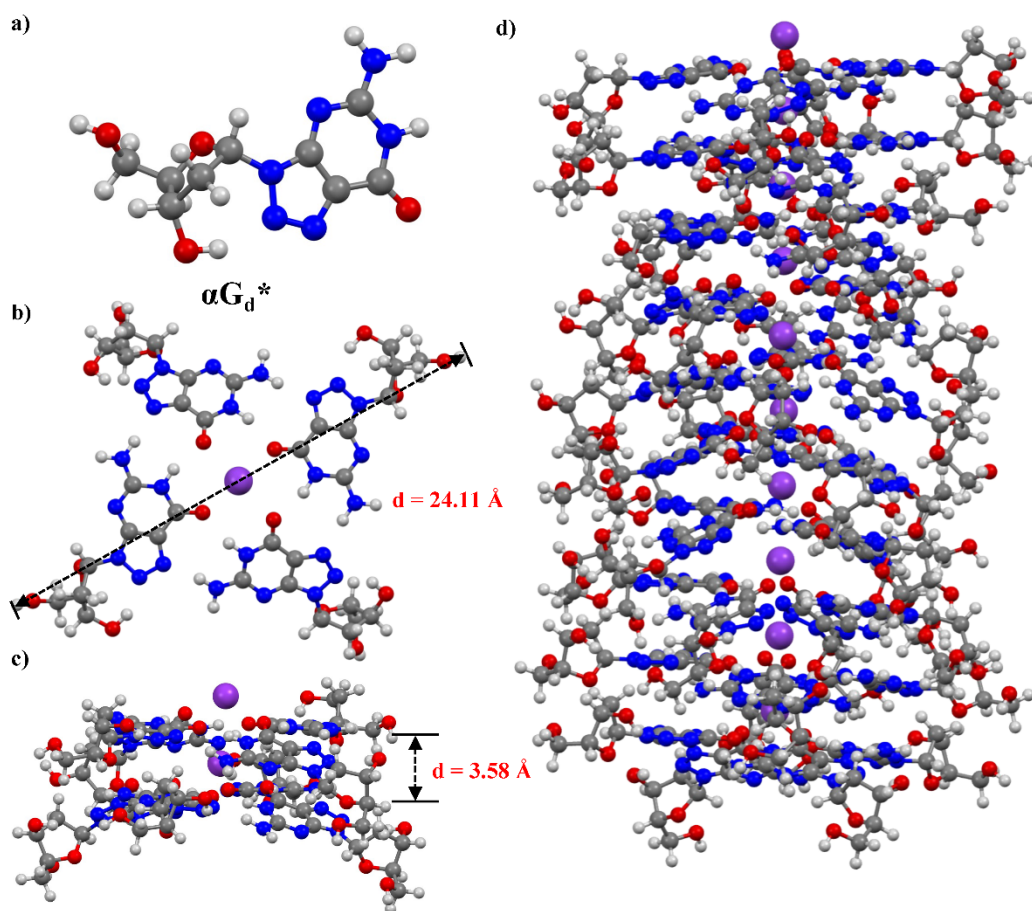
Figure S5. Structural modeling of various structures formed by **G**. a) the molecular structure of **G**. b) the G-quartet block structure under the mediation of potassium ions. c) the stacking structure formed by 2 layers of G-quartet blocks. d) the stacking structure composed of 10 layers of G-quartet blocks.
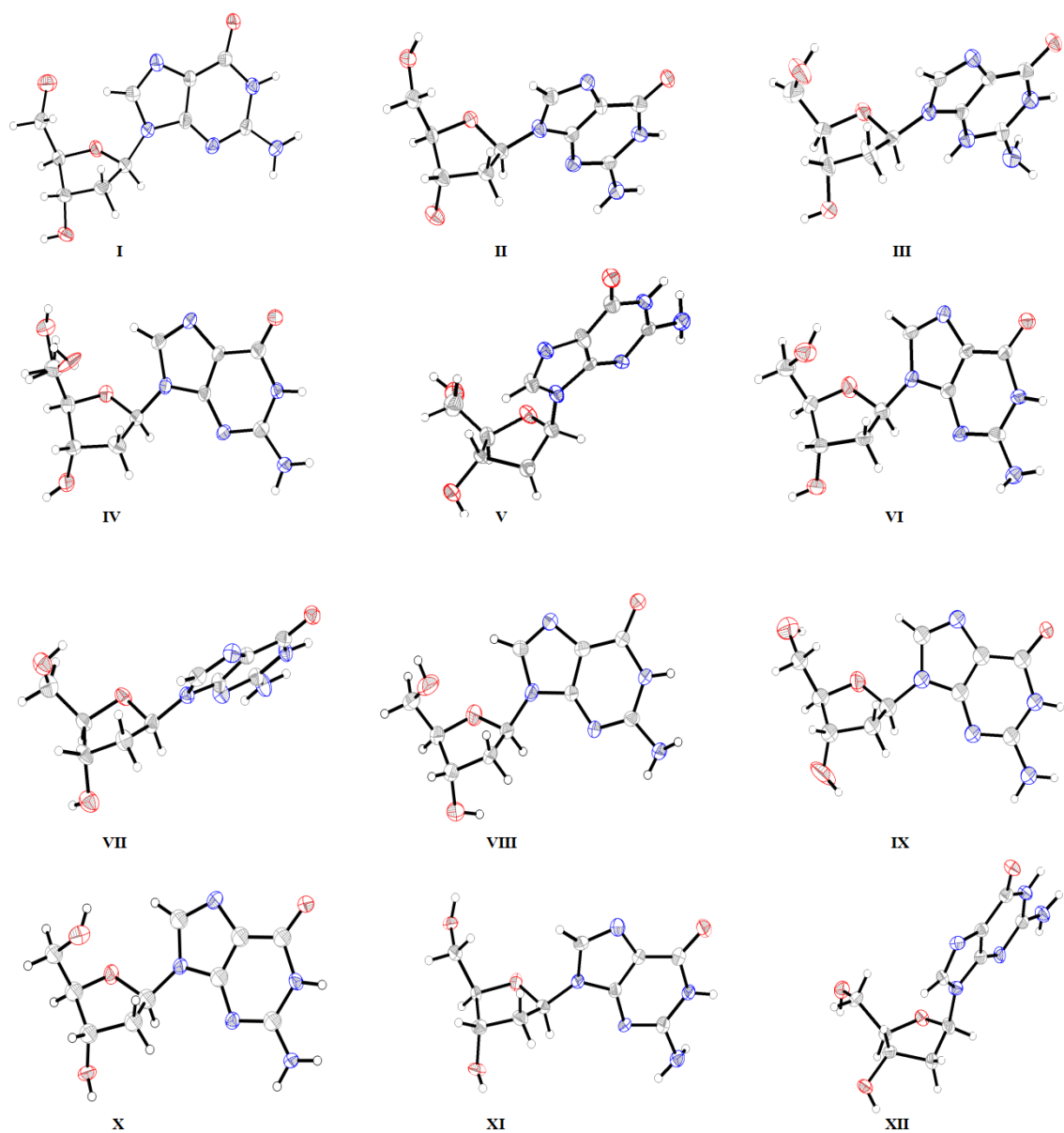
Figure S6. Structural modeling of various structures formed by **αG_d**. a) the molecular structure of **αG_d**. b) the G-quartet block structure under the mediation of potassium ions. c) the stacking structure formed by 2 layers of G-quartet blocks. d) the stacking structure composed of 10 layers of G-quartet blocks.

Figure S7. Structural modeling of various structures formed by **αG$_d$***. a) the molecular structure of **αG$_d$***. b) the G-quartet block structure under the mediation of potassium ions. c) the stacking structure formed by 2 layers of G-quartet blocks. d) the stacking structure composed of 10 layers of G-quartet blocks.
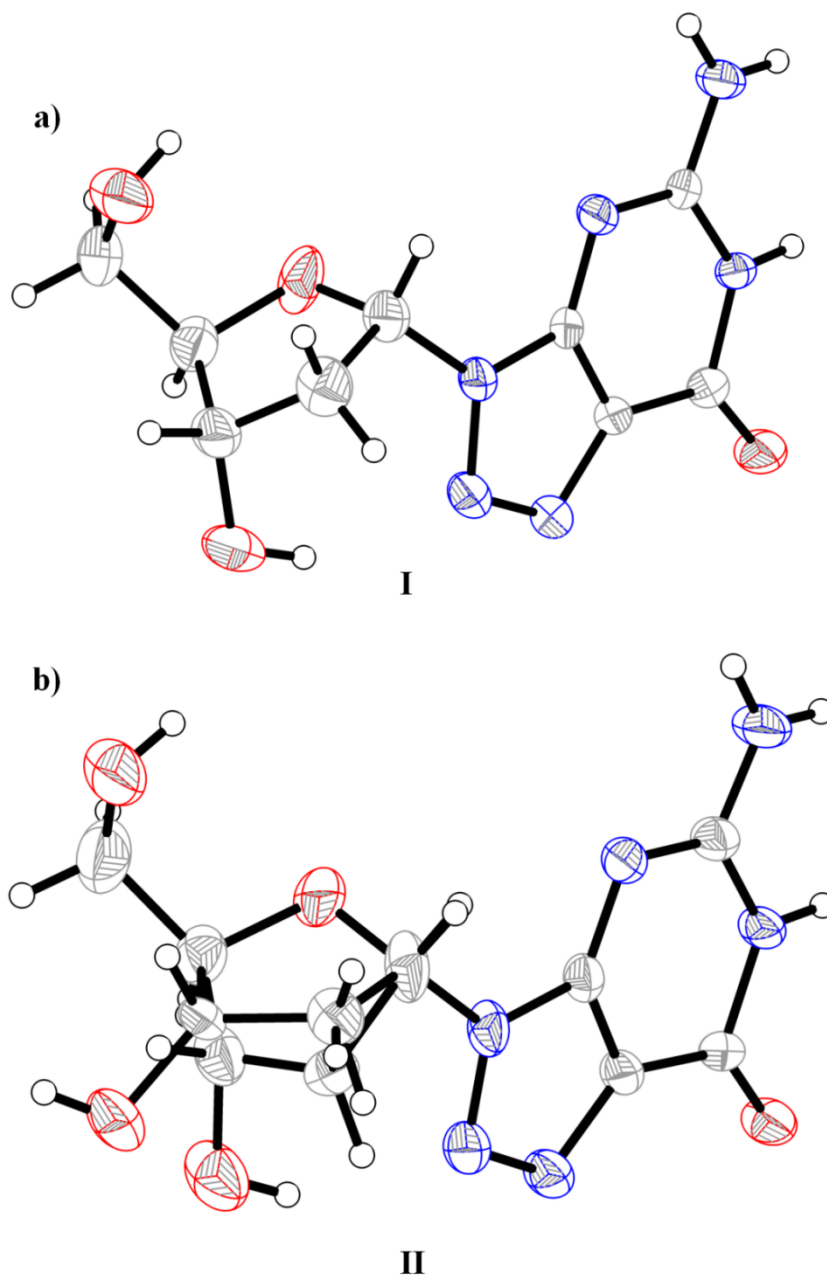
Figure S8. The single-crystal structures of **G_d** with 12 conformers from I to XII. C, N and O atoms were shown in Ellipsoid model, H atoms were shown in Global model.

a)

I

b)

II
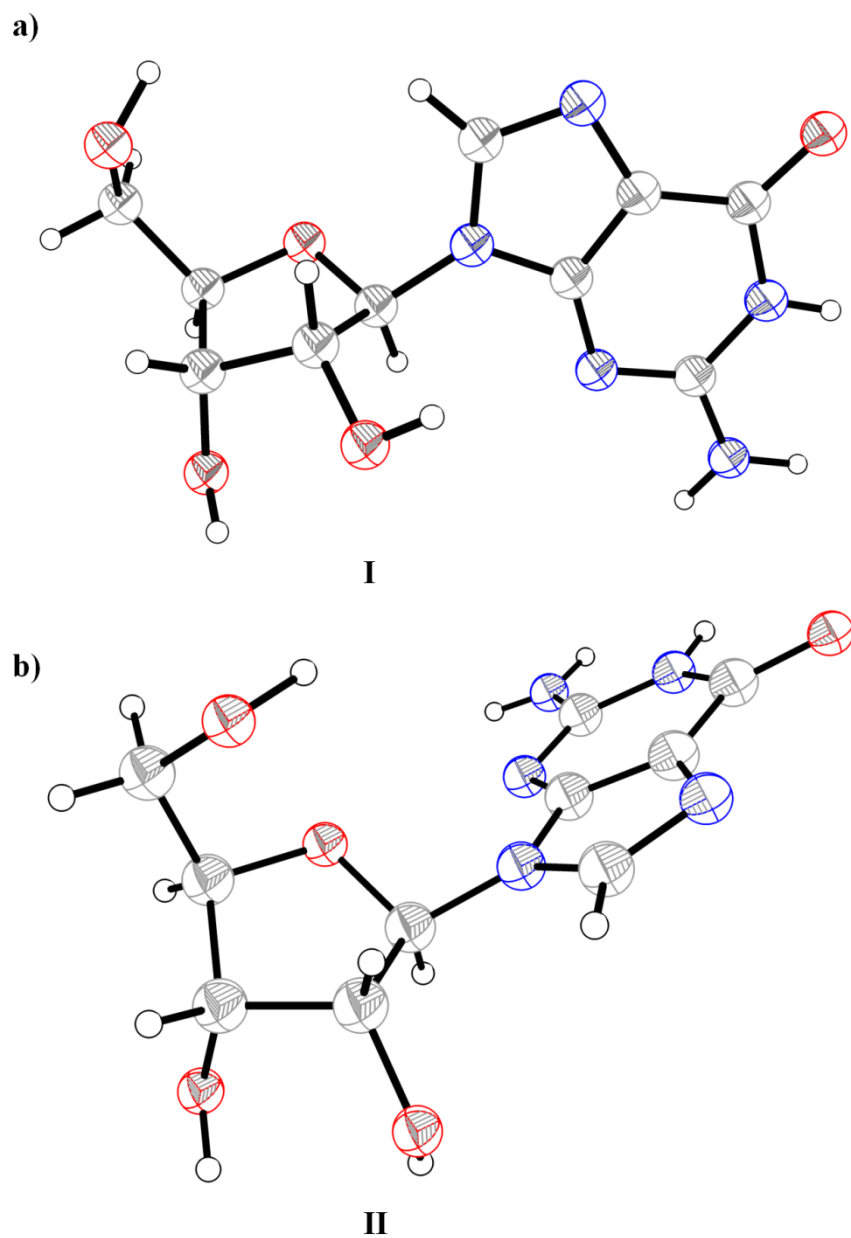
Figure S9. The single-crystal structures of **G** conformer I and II. X-ray single crystal data was got from reference,[3] atoms was shown in Ball and Stick Model.
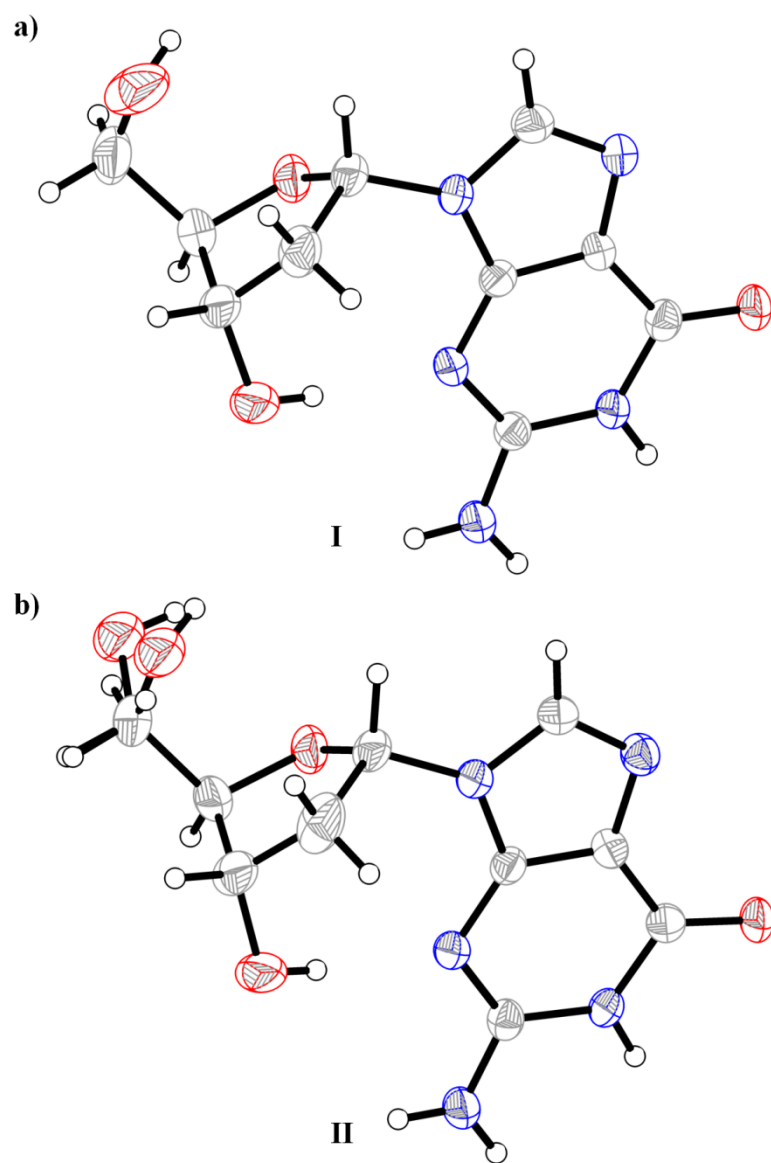
Figure S10. The single-crystal structures of **αG_d** conformer I and conformer II. Atoms are shown in Ellipsoid Model, there was two kinds of C2'-C3' bond in conformer II. Atoms are coded as follows: red, oxygen; blue, nitrogen; gray, carbon; white, hydrogen.

**Figure S11.** The single-crystal structures of **αG_d*** conformer I and conformer II. N, O, and C atoms were shown in Ellipsoid Model, H atoms were shown in Global. Atoms are coded as follows: red, oxygen; blue, nitrogen; gray, carbon; white, hydrogen.
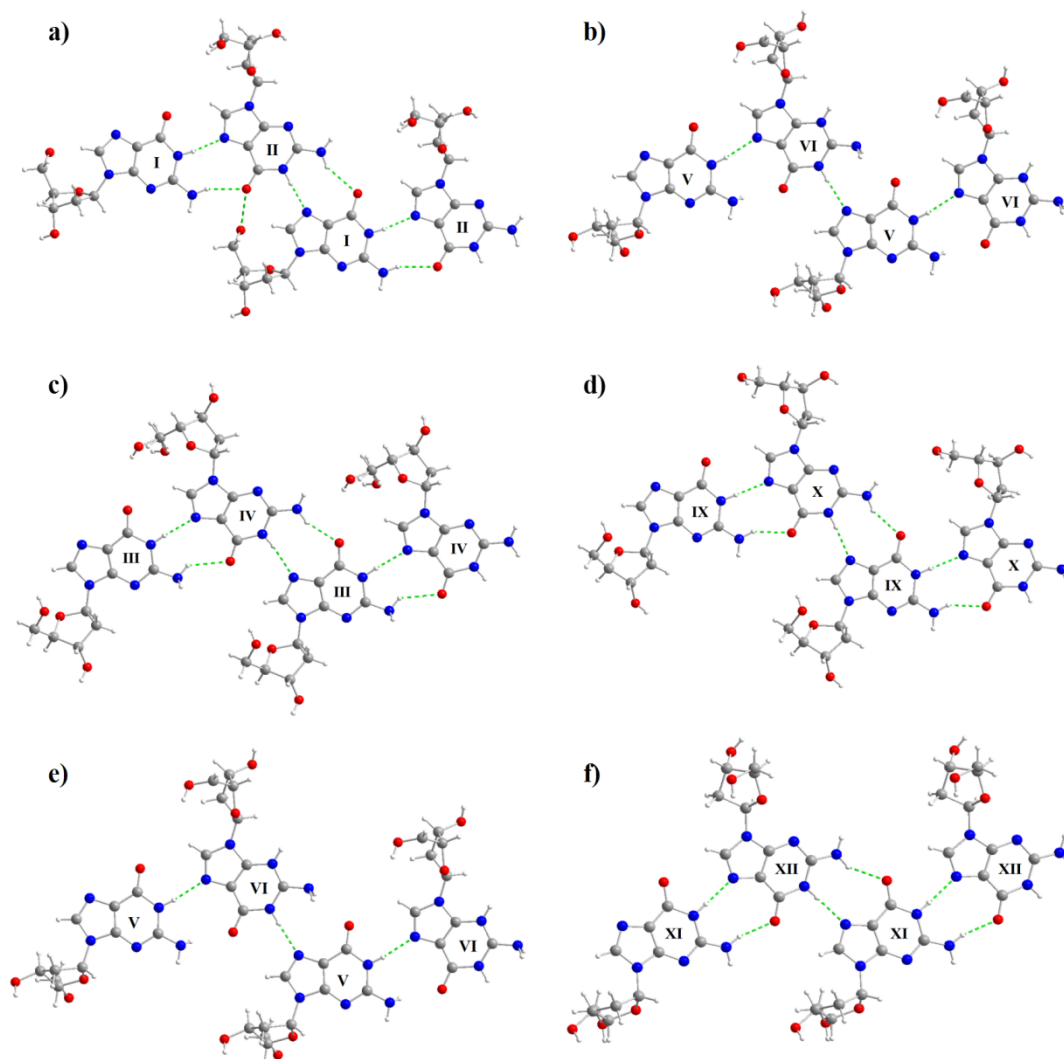
Figure S12. The base-pair pattern of **G_d** in the crystal. 6 base pairs show the same hydrogen bonds N1H---N7, N2H---O6. Atoms are coded as follows: red, oxygen; blue, nitrogen; gray, carbon; white, hydrogen.
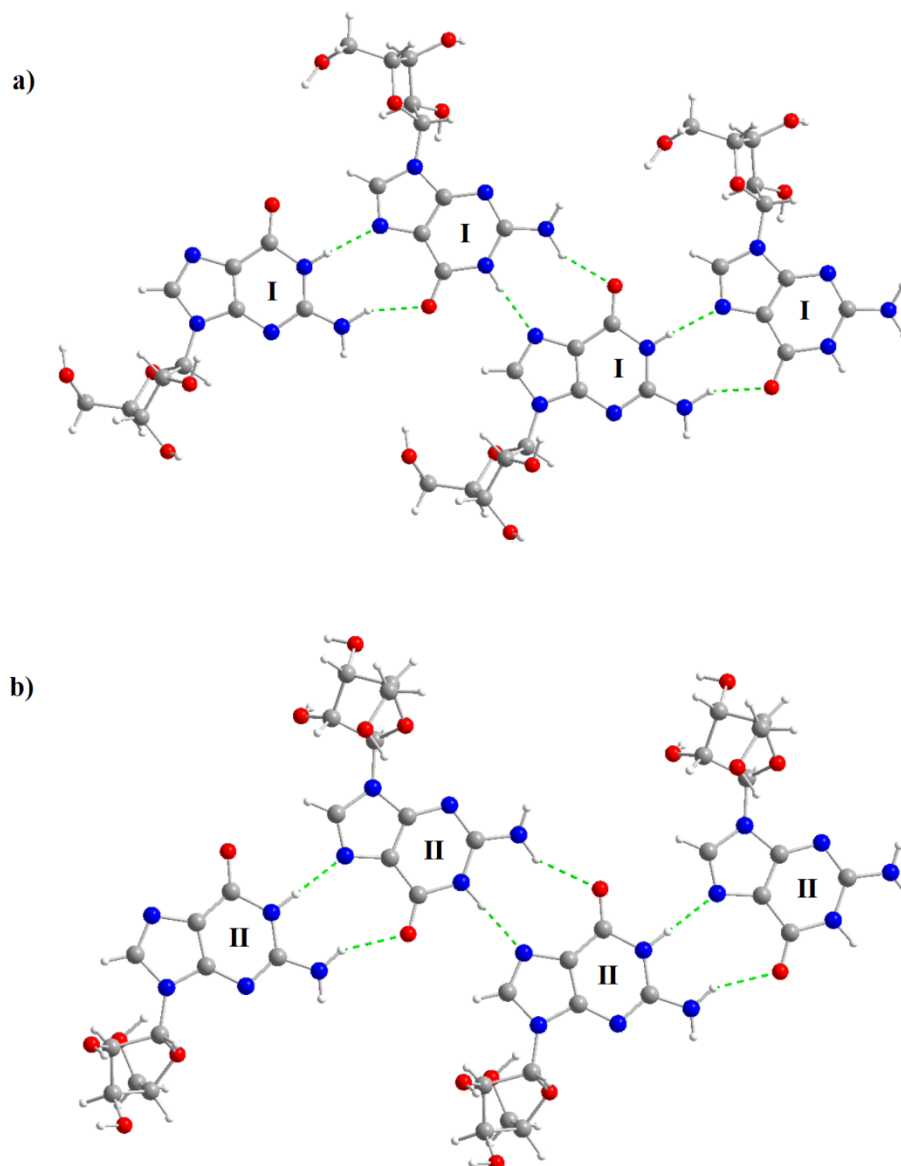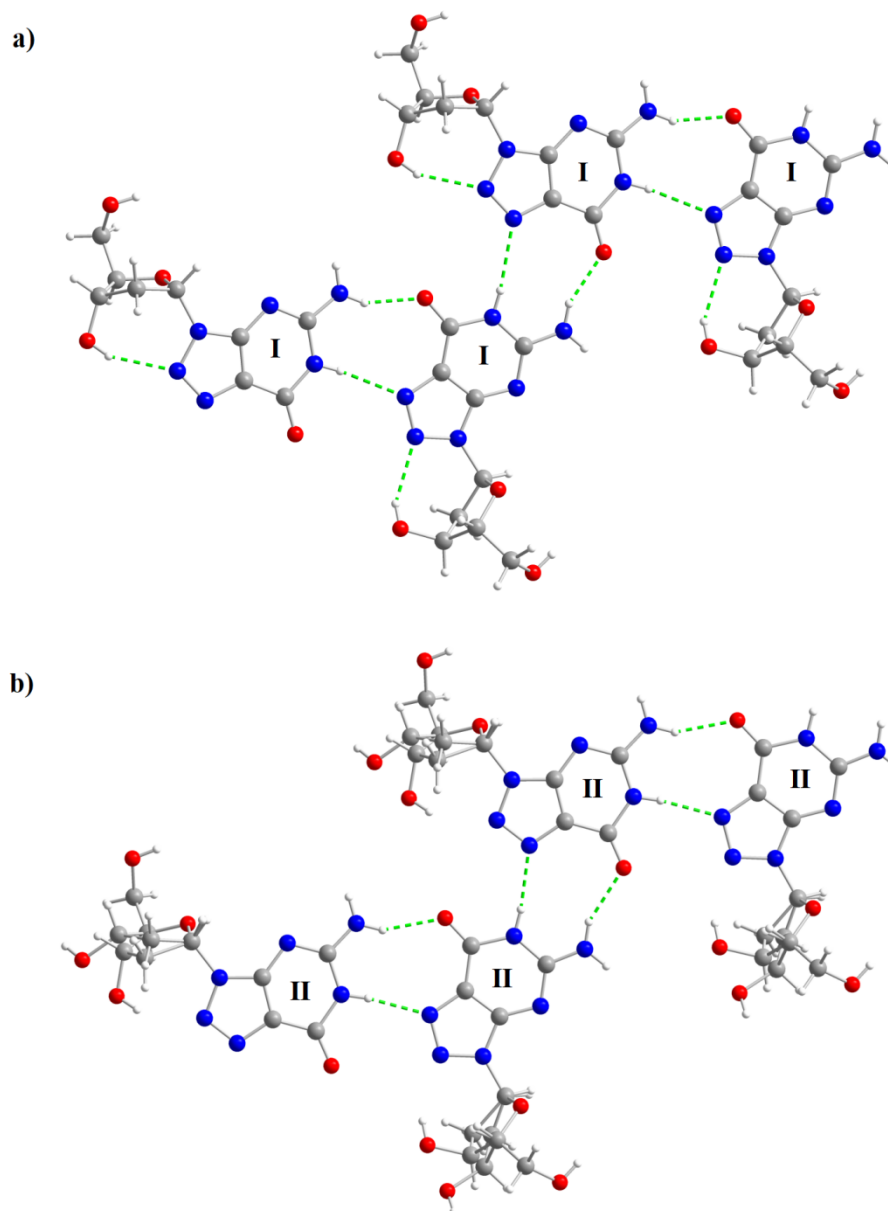
Figure S13. The base-pair pattern of **G** in the crystal. a) The repeated hydrogen bonds unit connecting conformers I; b) The repeated hydrogen bonds unit connecting conformers II. Atoms are coded as follows: red, oxygen; blue, nitrogen; gray, carbon; white, hydrogen.
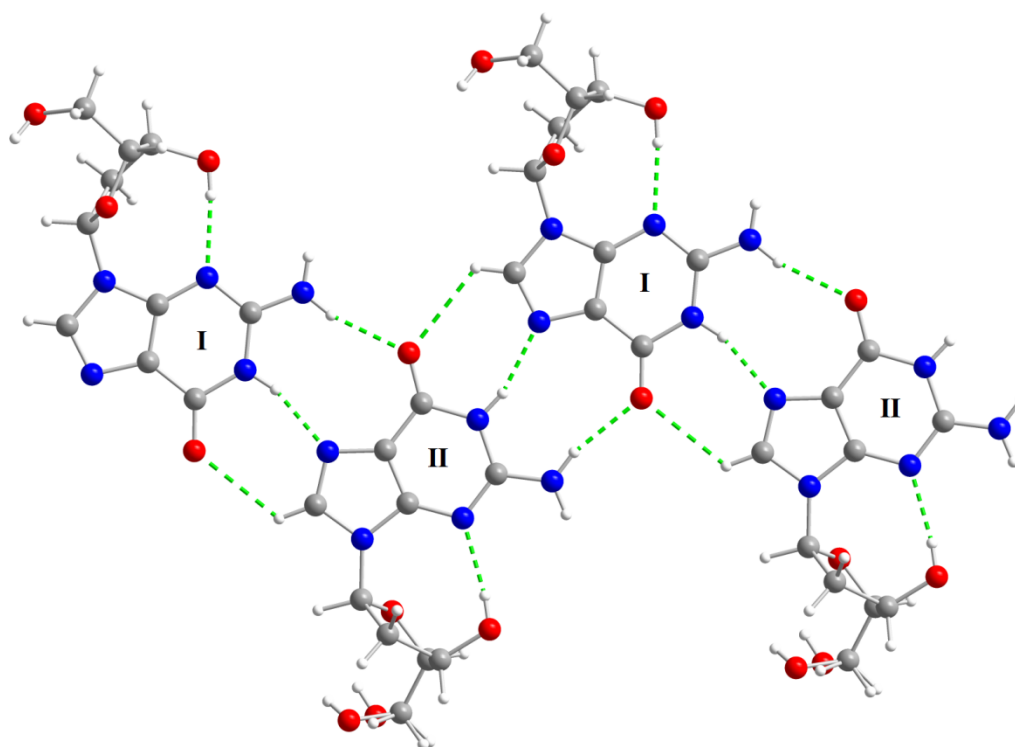
Figure S14. The base-pair pattern of **αG_d** in the crystal. With participating of hydrogen bond between C8 and O6, the two conformers formed triple hydrogen bond base pairs. The repeated hydrogen bonds unit connecting conformers I and II together in the whole assembly is highlighted in green color. Atoms are coded as follows: red, oxygen; blue, nitrogen; gray, carbon; white, hydrogen.

Figure S15. The base-pair pattern of **αG$_d$*** in the crystal. a) The repeated hydrogen bonds unit connecting conformers I; b) The repeated hydrogen bonds unit connecting conformers II. Atoms are coded as follows: red, oxygen; blue, nitrogen; gray, carbon; white, hydrogen.
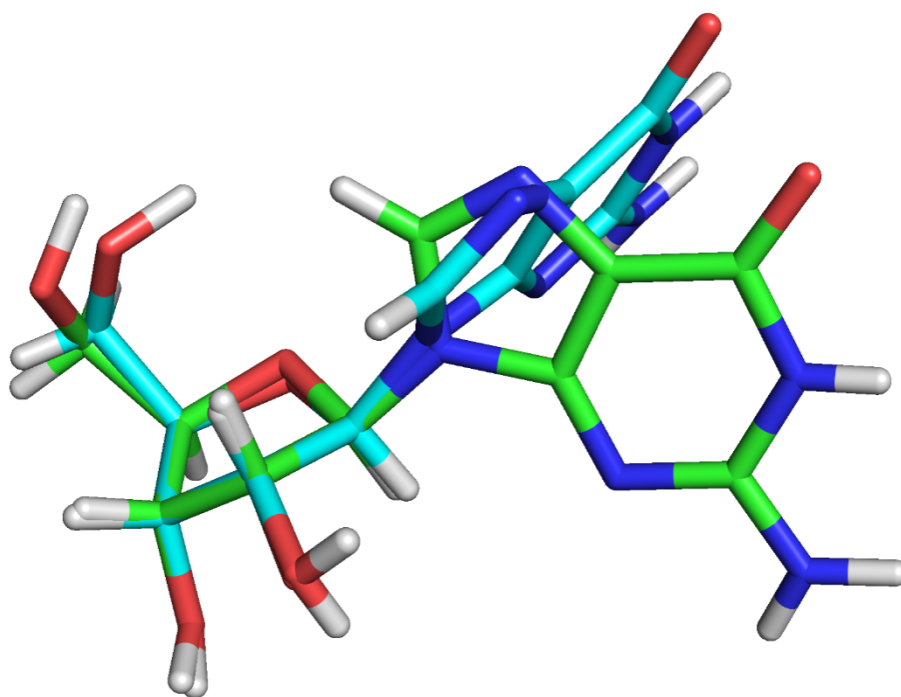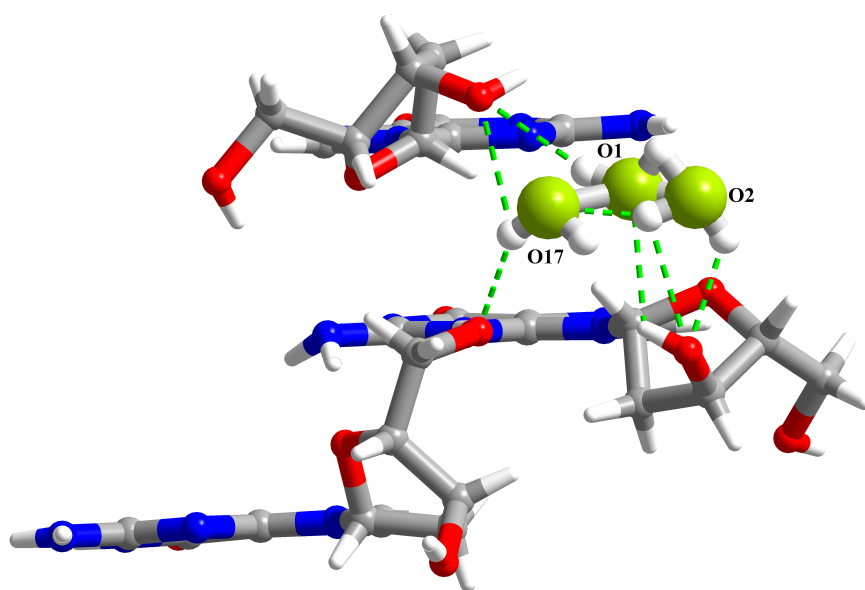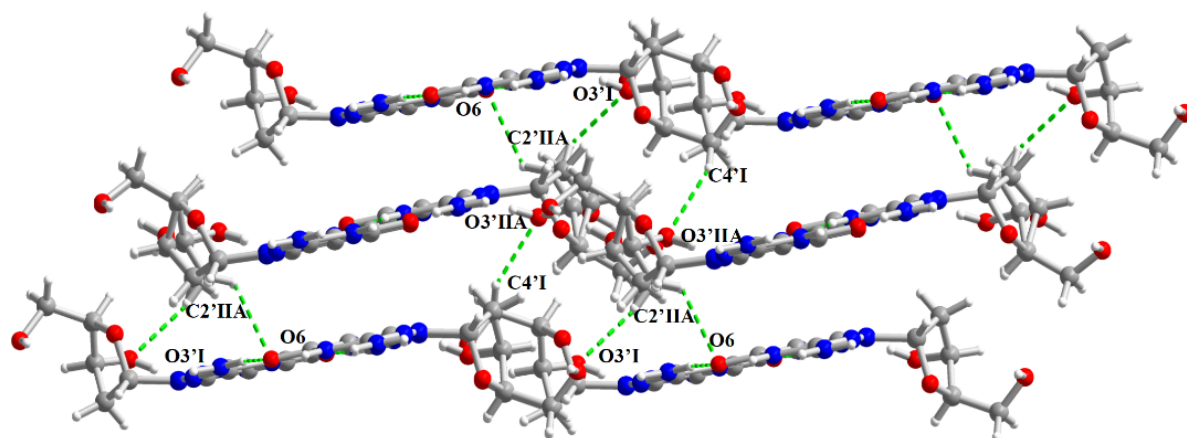
Figure S16. Sugar rings overlay results of two conformers of **G.**

Figure S17. Disordered water in the **G_d** crystal. Oxygen of water was shown in Lime. Hydrogen bond was shown in light green dash line.

Figure S18. Base layers crosslink in **αG_d*** crystal without water. The hydrogen bond C2'H(II)A---O6, C2'(II)H---O3'(I), C4'(I)H---O3'(II)A, connected the base layers. Hydrogen bonds was shown in bright green. Atoms are coded as follows: red, oxygen; blue, nitrogen; gray, carbon; white, hydrogen.
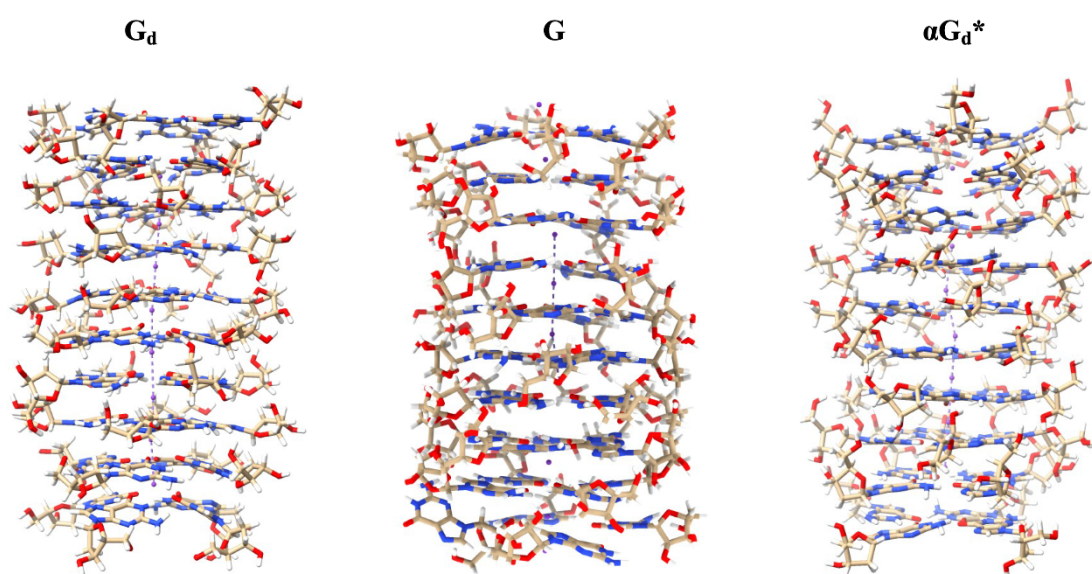
Figure S19. Snapshots of MD simulation ending state of **G_d**, **G** and **αG_d**.
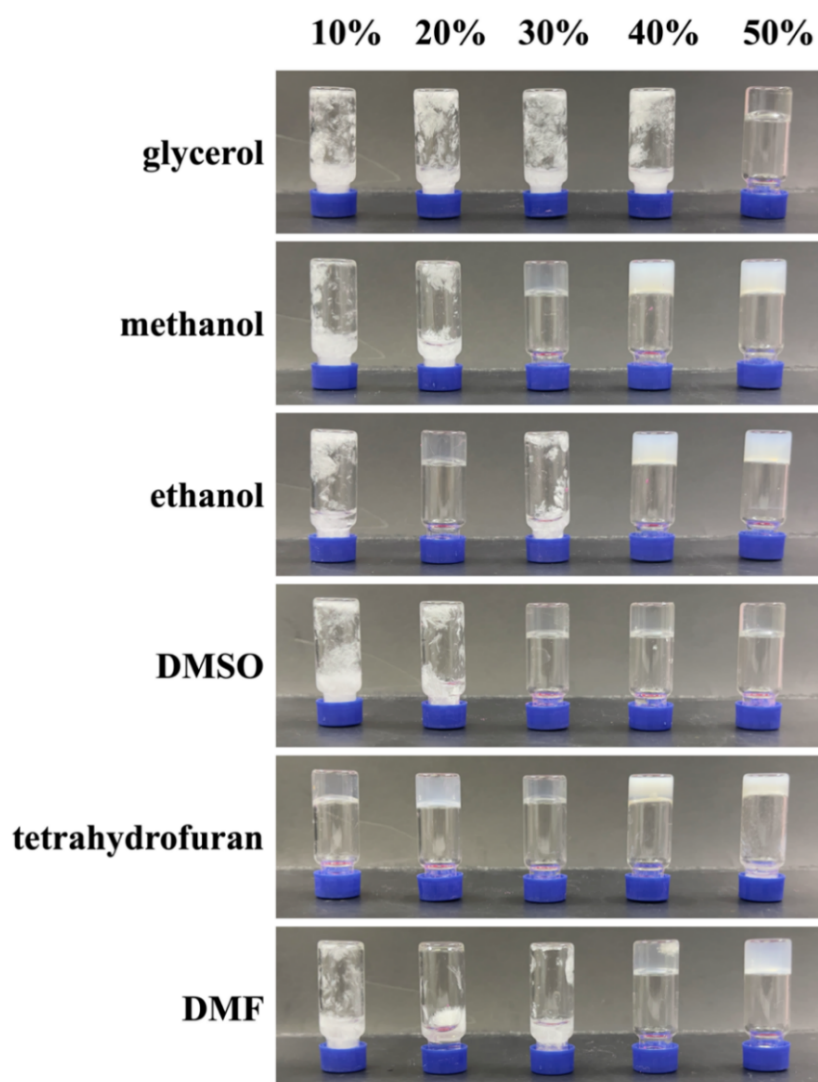
Figure S20. Gel formation of **G** in KCl solutions equipped with various organic solvents in different proportions. The concentration of **G** is 14 mg/mL and K^+ 0.2 mmol/mL in other analysis, The volume ratio of the organic solvent was varied from 10% to 50%.
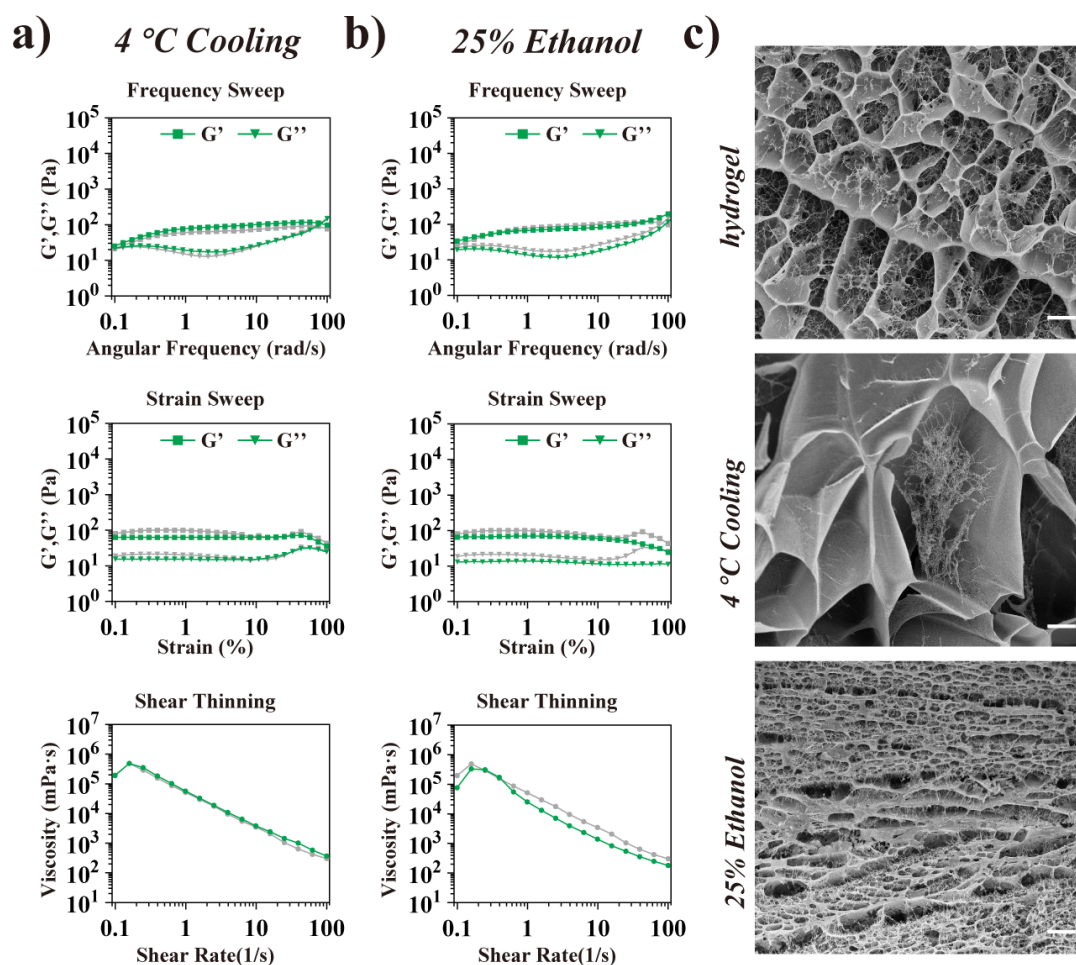
Figure S21. a-b) Rheological testing of αG$_d$ hydrogel prepared by the rapid cooling method (a) and organic solvents (b); the gray data represent the corresponding results for the hydrogels that without non-chemical modifications. c) Cryo-SEM imaging of the hydrogels prepared from **αG$_d$** by different methods. The concentration of **αG$_d$** is 14 mg/mL and the concentration of K$^+$ is 0.2 mmol/mL in the hydrogels. (Scale bar = 5 μm).

αGd*
(solution)
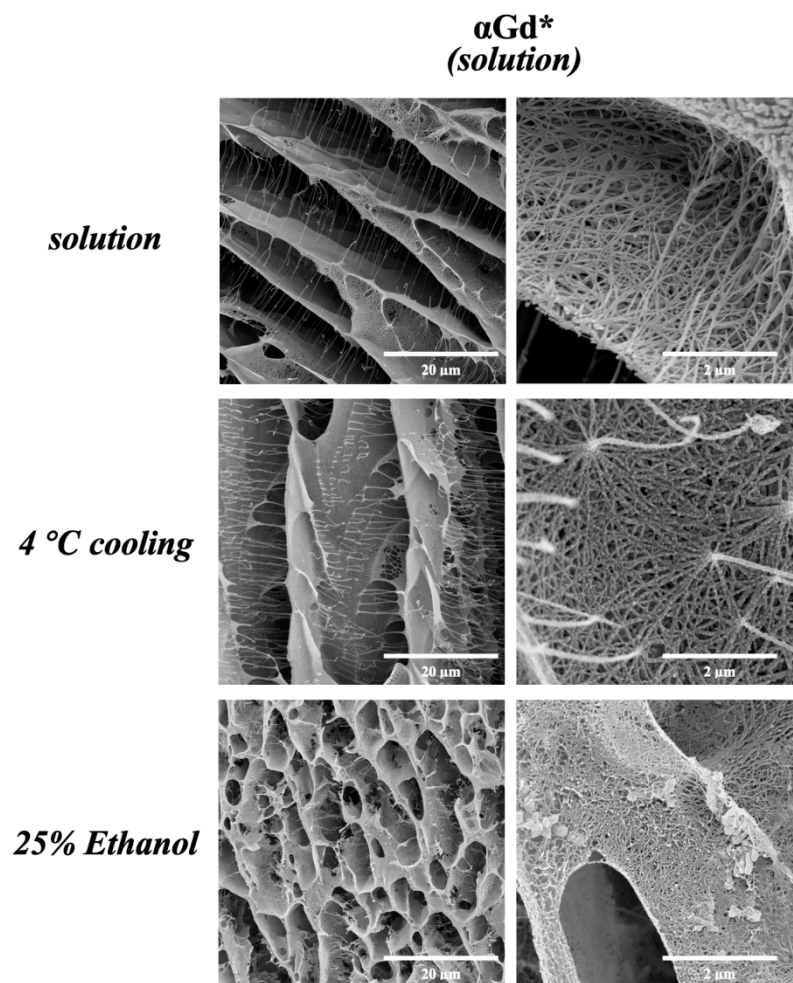
Figure S22. Cryo-SEM imaging of the **αG_d*** solution prepared by different methods. The concentration of **αG_d*** is 14 mg/mL and the concentration of K^+ is 0.2 mmol/mL in the solution.
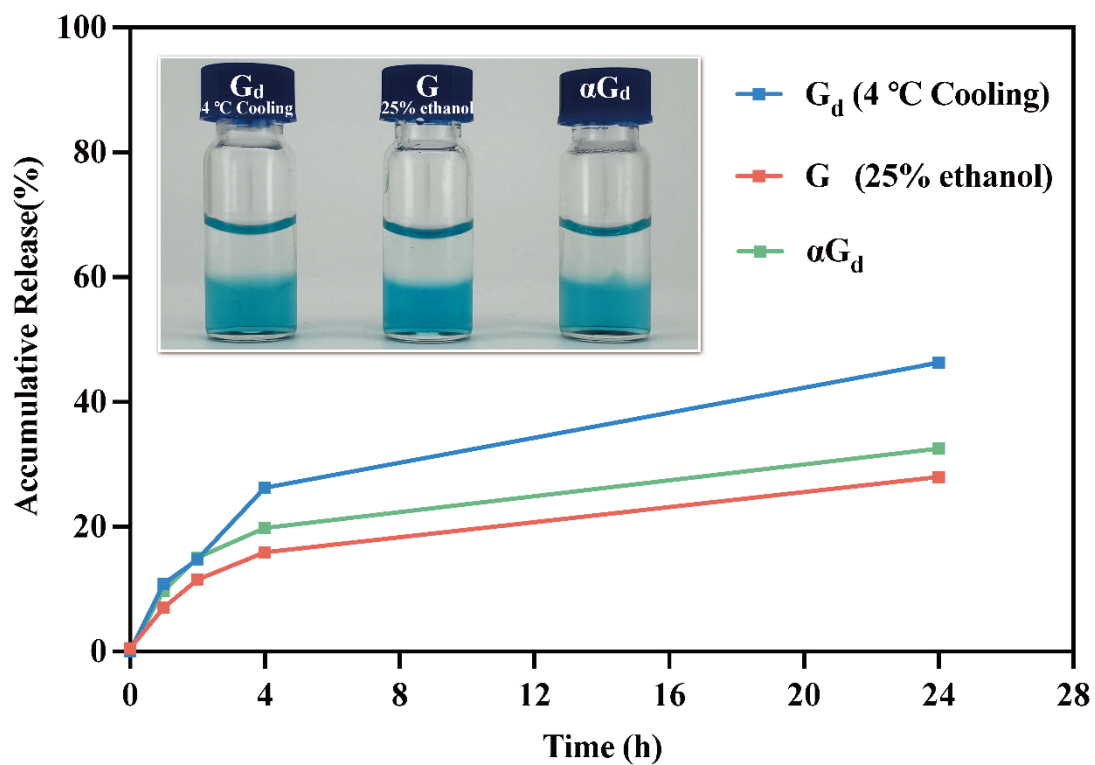
Figure S23. The methylene blue dye release experiment. The methylene blue within the hydrogels can be released slowly over a period of 24 hours. The concentration of G_d, G and αG_d is 14 mg/mL, the concentration of K^+ is 0.2 mmol/mL and the concentration of methylene blue is 0.4 µmol/mL.

Table S1. Summary of X-ray crystallographic data for compounds G_d, αG_d, and αG_d^*.

	G_d	αG_d	αG_d^*
Formula	$C_{60}H_{92}N_{30}O_{31}$ $(6C_{10}H_{13}N_5O_4 \cdot 7H_2O)$	$C_{10}H_{13.5}N_5O_{4.25}$ $(C_{10}H_{13}N_5O_4 \cdot 0.25H_2O)$	$C_9H_{12}N_6O_4$
FW	1729.63	271.76	268.25
Crystal system	triclinic	monoclinic	monoclinic
Space group	P1	C2	P2$_1$
a (Å)	10.6756(11)	10.9636(8)	9.092(5)
b (Å)	11.4060(12)	6.1525(5)	11.218(5)
c (Å)	33.093(3)	34.865(2)	11.613(6)
α (°)	85.849(3)	90	90
β (°)	87.833(3)	94.168(6)	101.827(12)
γ (°)	67.473(3)	90	90
Cell volume (Å^3)	3712.2(7)	2345.5(3)	1159.4(10)
Calc. density (g/cm^3)	1.547	1.539	1.537
Z	2	8	4
m (Mo-Kα)	0.71073	0.71073	0.71073
R$_{int}$	0.0356	0.0146	0.0466
R$_1$($I > 2\sigma(I)$)	0.0692	0.042	0.0635
wR$_2$	0.163	0.0929	0.1602
GOF	1.072	1.085	1.02
Temperature (K)	173	293.15	220
Wavelength (Å)	0.71073	0.71073	0.71073
Crystal size (mm)	0.05 × 0.04 × 0.02	0.35 × 0.3 × 0.25	0.08 × 0.03 × 0.01
μ (mm^{-1})	0.126	0.123	0.124
F(000)	1820	1140	560
Reflections with $I > 2\sigma(I)$	16511	5351	10294
Independent reflections	20262	3945	5218
CCDC.	2311975	2311973	2311972

Table S2. The length and angle of hydrogen bonds for base pairs in nucleoside crystals.

	N1H---N7	D----A (Å)	(D)H---A (Å)	<DHA (°)	N2H---O6	D----A (Å)	(D)H---A (Å)	<DHA (°)
	N1H(I)---N7(II)	2.7593	1.8844	172.399	N2H(I)---O6(II)	3.0277	2.1973	157.331
	N1H(II)---N7(I)	2.7307	1.8527	174.368	N2H(II)---O6(I)	3.0642	2.2565	152.560
	N1H(III)---N7(IV)	2.8225	1.9457	174.676	N2H(III)---O6(IV)	2.9518	2.2731	133.882
	N1H(IV)---N7(III)	2.9122	2.0410	170.786	N2H(IV)---O6(III)	2.9234	2.0865	158.686
	N1H(V)---N7(VI)	2.8864	2.0105	172.768	N2H(V)---O6(VI)[a]	2.8290	2.3846	111.550
	N1H(VI)---N7(V)	2.8778	2.0040	172.453	N2H(VI)---O6(V)[a]	2.8994	2.3770	118.240
G_d	N1H(VII)---N7(VIII)	2.8053	1.9264	176.585	N2H(VII)---O6(VIII)[a]	2.9536	2.5376	107.021
	N1H(VIII)---N7(VII)	2.7795	1.9006	177.100	N2H(VIII)---O6(VII)	2.9121	2.2693	129.523
	N1H(IX)---N7(X)	2.8235	1.9428	177.595	N2H(IX)---O6(X)	2.8953	2.1022	149.075
	N1H(X)---N7(IX)	2.8672	1.9898	175.356	N2H(X)---O6(IX)	2.872	2.0522	154.454
	N1H(XI)---N7(XII)	2.7913	1.9148	174.398	N2H(XI)---O6(XII)	2.8942	2.0601	162.019
	N1H(XII)---N7(XI)	2.8437	1.9729	169.664	N2H(XII)---O6(XI)	2.9372	2.1266	153.023
G	N1H(I)---N7(I)	2.8166	1.9513	175.262	N2H(I)---O6(I)	2.9179	2.0011	152.243
	N1H(II)---N7(II)	2.8759	1.9379	178.589	N2H(II)---O6(II)	2.9900	2.1451	151.181
αG_d	N1H(I)---N7(II)	2.7592	1.9263	162.901	N2H(I)---O6(II)	2.9028	2.0586	166.910
	N1H(II)---N7(I)	2.7516	1.9166	163.532	N2H(II)---O6(I)	2.9000	2.0589	165.940
αG_d*	N1H(I)---N7(I)	3.1489	2.2821	173.944	N2H(I)---O6(I)	2.7343	1.9249	154.153
	N1H(II)---N7(II)	2.9365	2.0744	171.117	N2H(II)---O6(II)	2.8590	2.0441	155.536

[a]As the angle of N2H---O6 or distance between the H to O6 didn't conform to normal hydrogen bonds, there is no hydrogen bonds between N2H---O6 in the crystals.

Table S3. Conformers and their conformation of G compounds in crystals.

Compounds	Conformers	γ^a (°) (O5'-C5'-C4'-C3')	χ^b (°) (O4'-C1'-N9-C4)	Orientation Model	Pseudorotation phase angle (°) (P)	Twist form
Gd	I	161.13	-112.19	*anti*	199.33	C3'-*exo*-C4'-*endo* ($_3T^4$)
	II	175.45	-111.73	*anti*	154.58	C2'-*endo*-C1'-*exo* ($^2T_1$)
	III	56.33	-179.21	*anti*	170.51	C2'-*endo*-C3'-*exo* ($^2T_3$)
	IV	178.43 46.39	-162.57	*anti*	195.90	C3'-*exo*-C2'-*endo* ($_3T^2$)
	V	-167.93	-87.27	*high anti*	6.01	C3'-*endo*-C2'-*exo* ($^3T_2$)
	VI	47.17	-90.12	*high anti*	146.51	C2'-*endo*-C1'-*exo* ($^2T_1$)
	VII	-176.30	-113.89	*anti*	159.91	C2'-*endo*-C1'-*exo* ($^2T_1$)
	VIII	49.68	-155.35	*anti*	181.19	C3'-*exo*-C2'-*endo* ($_3T^2$)
	IX	58.03	-178.84	*anti*	172.60	C2'-*endo*-C3'-*exo* ($^2T_3$)
	X	-175.34	-155.95	*anti*	147.24	C2'-*endo*-C1'-*exo* ($^2T_1$)
	XI	-161.94	-82.99	*high anti*	344.67	C2'-*exo*-C3'-*endo* ($_2T^3$)
	XII	43.99	-72.69	*high anti*	134.32	C1'-*exo*-C2'-*endo* ($_1T^2$)
G	I	46.44	-137.19	*anti*	138.37	C1'-*exo*-C2'-*endo* ($_1T^2$)
	II	67.94	-58.08	*syn*	161.01	C2'-*endo*-C1'-*exo* ($^2T_1$)
αGd	I	63.36	-57.87	*syn*	222.49	C4'-*endo*-C3'-*exo* ($^4T_3$)
	II	70.05 163.97	-58.12	*syn*	220.50	C4'-*endo*-C3'-*exo* ($^4T_3$)
αGd*	I	55.39	81.97	*high anti*	167.11	C2'-*endo*-C3'-*exo* ($^2T_3$)
	II	65.82 53.63	76.90	*high anti*	94.34 91.01	C1'-*exo*-O4'-*endo* ($^0T_1$) C1'-*exo*-O4'-*endo* ($^0T_1$)

[a]The torsion angle γ (O5'-C5'-C4'-C3') defined the 5'-OH toward the sugar ring; [b]The torsion angle of χ(O4'-C1'-N9-C4) range -90~+90° is denoted as *syn*, and range 180±90° is denoted as *anti*, most of these nucleoside conformers show *anti* conformation.

Table S4. The torsion angle of bonds in the sugar ring.

Compounds	Conformers	v_0 (°) (C4'-O4'-C1'-C2')	v_1 (°) (O4'-C1'-C2'-C3')	v_2 (°) (C1'-C2'-C3'-C4')	v_3 (°) (C2'-C3'-C4'-O4')	v_4 (°) (C3'-C4'-O4'-C1')
G_d	I	1.2289	20.2429	-32.8569	33.7548	-21.874
	II	-28.6577	40.7168	-36.6938	20.6538	4.9408
	III	-13.7009	26.4849	-28.3379	20.8579	-4.7519
	IV	-1.4438	20.4018	-30.3498	30.1058	-18.3398
	V	8.8439	-29.3108	37.7708	-34.0498	16.3479
	VI	-33.1969	42.1489	-34.3559	15.8811	10.4959
	VII	-24.5007	38.4827	-36.4628	22.9468	1.0018
	VIII	-10.3869	28.7839	-35.1089	29.4139	-11.9941
	IX	-17.3988	35.5307	-39.1497	29.5247	-7.7508
	X	-27.2671	34.9101	-28.5261	13.7791	8.1011
	XI	20.2198	-34.7338	34.6938	-23.4018	2.2728
	XII	-39.8978	43.3518	-30.2019	7.5749	19.5048
G	I	-38.5202	44.2422	-32.4092	11.0762	16.9872
	II	-22.0542	34.7422	-33.3912	21.9542	0.1692
αG_d	I	13.1194	7.0404	-22.9514	30.8264	-27.8014
	II	11.7224	7.9474	-23.1254	30.3224	-26.6804
$\alpha G_d{}^*$	I	-14.1506	25.4136	-26.0826	18.3446	-2.8446
	II	-10.6307	6.9191	-0.8072	-5.3352	9.8201
		-31.3530	18.9832	-0.5712	-17.8861	31.9578

Table S5 The bond length and bond angle of water moleculars in nucleoside crystals.

Compounds	Number of H₂O	Bond length (Å)	Bond angle(°)
	H₂O(1)	- -	-
	H₂O (2)	- -	-
	H₂O (3)	0.8695 0.8704	104.492
	H₂O (4)	0.8707 0.8693	109.469
	H₂O (5)	0.8697 0.8709	104.457
	H₂O (6)	0.8712 0.8693	104.552
	H₂O (7)	0.8702 0.8705	104.493
	H₂O (8)	0.8699 0.8709	104.490
G_d	H₂O (9)	0.8701 0.8705	109.457
	H₂O (10)	0.8703 0.8695	104.563
	H₂O (11)	0.8705 0.8696	104.560
	H₂O (12)	0.8709 0.8698	104.440
	H₂O (13)	0.8706 0.8688	109.661
	H₂O (14)	0.8705 0.8693	109.480
	H₂O (15)	0.8712 0.8687	104.525
	H₂O (16)	0.8692 0.8694	104.618
	H₂O (17)	- -	-
	H₂O (1)	0.9063 0.8611	114.615
	H₂O (2)	0.9169 0.7988	104.179
G	H₂O (3)	0.9177 0.9121	99.203
	H₂O (4)	0.8729 0.8860	109.739
αG_d	H₂O (1)	0.7993 0.7993	79.338

Reference

S1. J. Liu, S. A. Ingale and F. Seela, Guanine and 8-azaguanine in anomeric DNA hybrid base pairs: stability, fluorescence sensing and efficient mismatch discrimination with α-D-nucleosides, *Bioconjugate Chem.,* 2018, *29*, 2265-2277.

S2. X.-Q. Xie, Y. Zhang, Y. Liang, M. Wang, Y. Cui, J. Li, and C.-S. Liu, Programmable transient supramolecular chiral G-quadruplex hydrogels by a chemically fueled non-equilibrium self-Assembly strategy, *Angew. Chem. Int. Ed. Engl.,* 2022, **61**, e202114471.

S3. U. Thewalt, C. E. Bugg and R. E. Marsh, The crystal structure of guanosine dihydrate and inosine dihydrate, *Acta cryst.,* 1970, **B26**, 1089-1101.